

## INTERACTING GALAXIES HIDING INTO ONE, REVEALED BY MANGA

B. Mazzilli Ciraulo<sup>1</sup>, A.-L. Melchior<sup>1</sup>, D. Maschmann<sup>1,3</sup>, I. Y. Katkov<sup>2,3,4</sup>, A. Hallé<sup>1</sup>, F. Combes<sup>1,5</sup>,  
J. D. Gelfand<sup>2,3,6</sup> and A. Al Yazeedi<sup>2,3</sup>

### Abstract.

Interacting galaxies represent a fundamental tool for investigating the underlying mechanisms that drive galaxy evolution. In order to identify merging systems, high-resolution spectroscopic data are required, especially when the morphology does not show clear galaxy pairs. Here, we present a merging galaxy, MaNGA 1-114955, in which we highlighted the superimposition of two distinct rotating discs along the line of sight. We suggest that we are observing a pre-coalescence stage of a merger. Our results demonstrate how a galaxy can hide another one and the relevance of a multi-component approach for studying ambiguous systems.

Keywords: Galaxy: evolution – Galaxy: kinematics and dynamics – Galaxies: interactions – Techniques: spectroscopy – Methods: data analysis

## 1 Introduction

The improvement in data resolution has made it possible to highlight various observational signatures of mergers, such as colour change (Alonso et al. 2012), morphological disruption (Casteels et al. 2013), star formation enhancement (Patton et al. 2013), and merger-induced nuclear activity at low redshift for optical and mid-IR active galactic nuclei (AGN; Ellison et al. 2019). The presence of double nuclei (such as in NGC 3526; Sakamoto et al. 2014) is a clear signature of mergers as the existence of tidal tails (Mesa et al. 2014) and, alternatively, spectral features, such as double-peaked profiles in molecular gas emission lines, have also been interpreted as merger signatures (e.g. Greve et al. 2005; Weiß et al. 2005).

The galaxy merger studied here consists of a system at  $z = 0.09$  which belongs to a sub-sample (Mazzilli Ciraulo et al., in prep.) created by cross-identifying the MaNGA data release (SDSS DR15, Aguado et al. 2019) and a catalogue gathering sources with detected double-peaked emission-line profiles in their central SDSS spectrum (Maschmann et al. 2020).

## 2 Unveiling a merger event through a multi-component decomposition

### 2.1 Gas kinematics from the multi-component approach

We developed a two-component fitting procedure that we applied to the main emission lines in all the binned spectra of the MaNGA data. We highlighted two components along the line of sight, separated by a velocity difference  $\Delta V \sim 450 \text{ km s}^{-1}$ . The first object is a galaxy with a fairly regular velocity field, whereas the second is detected in a smaller region of the field of view, shows a slightly stronger  $H\alpha$  line flux, and shows a velocity field counter-rotating with respect to the main object. The 2D maps are displayed on Fig. 1.

<sup>1</sup> LERMA, Sorbonne Université, Observatoire de Paris, Université PSL, CNRS, F-75014, Paris, France

<sup>2</sup> New York University Abu Dhabi, Saadiyat Island, PO Box 129188, Abu Dhabi, UAE

<sup>3</sup> Center for Astro, Particle, and Planetary Physics, NYU Abu Dhabi, PO Box 129188, Abu Dhabi, UAE

<sup>4</sup> Sternberg Astronomical Institute, M.V. Lomonosov Moscow State University, 13 Universitetsky prospect, Moscow, 119991, Russia

<sup>5</sup> Collège de France, 11 Place Marcelin Berthelot, 75005 Paris, France

<sup>6</sup> Center for Cosmology and Particle Physics, New York University, 726 Broadway, New York, NY 10003, US

## 2.2 Consistent gas and star kinematics

We found associated counterparts to the gaseous double-peaked structure in the stellar kinematics, using an analysis workflow based on the full spectral fitting technique NBURSTS. We spotlighted two stellar population components: One is regular, and the second is less prominent but is detected in the region where we see a second gas component as well.

## 2.3 Figures

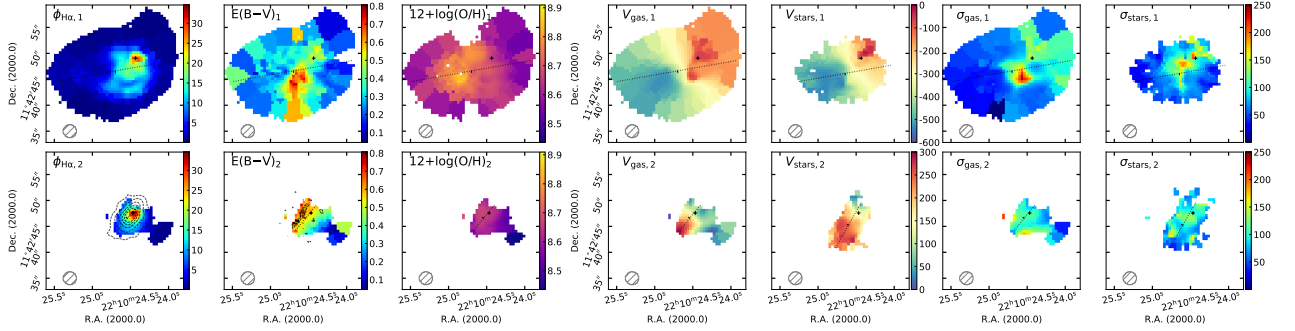


**Fig. 1.** The first and second rows show the maps for the first and second components detected in MaNGA data, respectively. **Left:** Gas properties derived from our fitting procedure. From left to right:  $H\alpha$  extinction-corrected flux (in  $\text{ergs}^{-1} \text{\AA}^{-1} \text{cm}^{-2}$  per spaxel), extinction computed from the Balmer decrement, and oxygen gas-phase abundance derived using the  $\text{O}_3\text{N}_2$  calibrator. The MaNGA PSF is displayed as a hatched grey circle in the bottom-left corner of the panels. **Right:** Kinematics of the gas and stars. First and second columns: respective ionised gas and stellar velocity fields (in  $\text{km s}^{-1}$ ). The dotted black lines refer to the computed position angles. Third and fourth columns: respective velocity dispersion fields (in  $\text{km s}^{-1}$ ) for the gas and the stars. As in the left panels, the black crosses indicate the position of the extinction-corrected  $H\alpha$  flux peak for the represented component.

## 3 Conclusions and remaining questions

Through the kinematics analysis of MaNGA 1-114955, we detected two separate components along the line of sight, both in gas and stars. We estimated a mass ratio of 9:1 between both objects. The second component shows an extended radio emission, that could be associated to the composite excitation of the gas observed within the system. The  $H\alpha$ -based star formation rate is under-estimated with respect to the one expected from the radio luminosity. From CO observations, we inferred an  $H_2$  mass corresponding to 21% of the total stellar mass. These results are detailed in the A&A accepted paper Mazzilli Ciraulo et al. (2021). High-resolution CO observations are in progress to get the kinematics of the molecular gas.

## References

- Aguado, D. S., Ahumada, R., Almeida, A., et al. 2019, *ApJS*, 240, 23  
 Alonso, S., Mesa, V., Padilla, N., & Lambas, D. G. 2012, *A&A*, 539, A46  
 Casteels, K. R. V., Bamford, S. P., Skibba, R. A., et al. 2013, *MNRAS*, 429, 1051  
 Ellison, S. L., Viswanathan, A., Patton, D. R., et al. 2019, *MNRAS*, 487, 2491  
 Greve, T. R., Bertoldi, F., Smail, I., et al. 2005, *MNRAS*, 359, 1165  
 Maschmann, D., Melchior, A.-L., Mamon, G. A., Chilingarian, I. V., & Katkov, I. Y. 2020, *A&A*, 641, A171  
 Mazzilli Ciraulo, B., Melchior, A.-L., Maschmann, D., et al. 2021, arXiv e-prints, arXiv:2106.07060  
 Mesa, V., Duplancic, F., Alonso, S., Coldwell, G., & Lambas, D. G. 2014, *MNRAS*, 438, 1784  
 Patton, D. R., Torrey, P., Ellison, S. L., Mendel, J. T., & Scudder, J. M. 2013, *MNRAS*, 433, L59  
 Sakamoto, K., Aalto, S., Combes, F., Evans, A., & Peck, A. 2014, *ApJ*, 797, 90  
 Weiß, A., Downes, D., Walter, F., & Henkel, C. 2005, *A&A*, 440, L45